Influence of the Solvent Evaporation Rate on the Crystalline Phases of Solution-Cast Poly(Vinylidene Fluoride) Films

Dante Luis Chinaglia,[1,2] Rinaldo Gregorio, Jr.,[3] Josiani Cristina Stefanello,[1] Ruy Alberto Pisani Altafim,[2,4] Werner Wirges,[2] Feipeng Wang,[2] Reimund Gerhard[2]

[1]*Department of Physics, Paulista State University "Júlio de Mesquita Filho" Rio Claro-SP, Brazil*
[2]*Department of Physics and Astronomy, Applied Condensed-Matter Physics, Faculty of Science, University of Potsdam, Potsdam, Germany*
[3]*Department of Materials Engineering, Federal University of São Carlos, São Carlos-SP, Brazil*
[4]*Department of Electrical Engineering, Engineering School of São Carlos, University of São Paulo, São Carlos-SP, Brazil*

Received 2 July 2009; accepted 21 September 2009
DOI 10.1002/app.31488
Published online 10 December 2009 in Wiley InterScience (www.interscience.wiley.com).

ABSTRACT: The influence of the solvent-evaporation rate on the formation of α and β crystalline phases in solution-cast poly(vinylidene fluoride) (PVDF) films was systematically investigated. Films were crystallized from PVDF/*N*,*N*-dimethylformamide solutions with concentrations of 2.5, 5.0, 10, and 20 wt % at different temperatures. During crystallization, the solvent evaporation rate was monitored *in situ* by means of a semianalytic balance. With this system, it was possible to determine the evaporation rate for different concentrations and temperatures of the solution under specific ambient conditions (pressure, temperature, and humidity). Fourier-Transform InfraRed spectroscopy with Attenuated Total Reflectance revealed the β-phase content in the PVDF films and its dependence on previous evaporation rates. Based on the relation between the evaporation rate and the PVDF phase composition, a consistent explanation for the different amounts of β phase observed at the upper and lower sample surfaces is achieved. Furthermore, the role of the sample thickness has also been studied. The experimental results show that not only the temperature but also the evaporation rate have to be controlled to obtain the desired crystalline phases in solution-cast PVDF films. © 2009 Wiley Periodicals, Inc. J Appl Polym Sci 116: 785–791, 2010

Key words: FT-IR; nucleation; poly(vinylidene fluoride); (PVDF); polymorphism; evaporation rate

INTRODUCTION

Mainly in view of their piezo- and pyroelectric properties, poly(vinylidene fluoride) (PVDF) and some of its copolymers are used in several practical device applications.[1,2] PVDF has a relatively simple chemical composition, lying between those of polyethylene and of polytetrafluoroethylene, which not only provides its molecular chain with high flexibility but also leads to some stereochemical constraints. The large difference in electronegativity between fluorine and hydrogen leads to a permanent electric dipole moment of the monomer unit that is approximately perpendicular to the chain axis. PVDF can be made piezo-, pyro-, and ferroelectric with an adequate sequence of processing steps. It is a semicrystalline polymer with at least four crystalline phases, the amount of which depends on the particular preparation conditions and which are usually labeled as α, β, γ, and δ.[3]

The nonpolar α phase is kinetically favored and may be obtained directly from the melt. In the α phase, the chains adopt a helical *trans*-gauche (TG^+TG^-) conformation, allowing a larger separation between fluorine atoms.[4] Although more difficult to obtain, the polar β phase is the most interesting from a technological point of view because of its strong piezo-, pyro-, and ferroelectric properties, as the chains adopt a planar zig-zag (all-trans or TTTT) conformation with a dipole moment of 2.1 D (Debye units, 1.0 D = 3.33564×10^{-30} C m) per monomer unit. Investigations of the crystallization process and of its dependence on temperature, on time, and on the nature of the solvent indicate that the β phase is thermodynamically more favorable. Conversion from the α into the β phase may achieved along

Correspondence to: D. L. Chinaglia (dantelc@rc.unesp.br).
Contract grant sponsors: CNPq, Fundunesp, INEO/CNPq, University of Potsdam, Germany, and EU, German Academic Exchange Service; contract grant number: DAAD, PROBRAL, D/08/11608

several routes that include mechanical stretching,[5,6] application of high electric fields in the solid state,[7] quenching directly from the melt,[8] and crystallization from solution at low temperatures.[9]

Preparation of a PVDF sample normally leads to more than one crystalline phase, in addition to an amount of amorphous phase. Significant efforts have been made to obtain a specific polymorph under reproducible, well-controlled conditions. For sample preparation from solution, for instance, the overall morphology may be controlled by adjusting the temperature, the type of solvent, the ambient conditions, and the solution concentration.[9–14] Gregorio and Borges[10] studied the effect of solvents with different boiling points at several different temperatures on the formation of the α and β phases during crystallization from solution. The amount of crystalline phases in PVDF was found to depend on the crystallization rate, which in turn depends on the solvent evaporation rate. Low evaporation rates favored formation of the β phase, whereas high rates resulted mainly in the α phase.

Because of the myriad of conditions and parameters affecting the formation of distinct phases in PVDF, a fine control is still lacking. Most authors have concentrated on the temperature as a single parameter to exert control, but in this article, we show that the evaporation rate may play an even more important role. To this end, we systematically investigated the crystallization of PVDF in *N*,*N*-dimethylformamide (DMF) solutions. The evaporation rate, *R*, at various concentrations was determined *in situ* at different crystallization temperatures and solution concentrations. The influence of the evaporation rate on the resulting crystalline phases and on the phase distribution across the sample thickness is also discussed.

EXPERIMENTAL DETAILS

Solutions were prepared by dissolving PVDF powder (Solvay®, 1000LD706S10) in *N*,*N*-DMF (Roth 99.9%) to concentrations of 2.5, 5.0, 10.0, and 20.0 wt % (close to the critical concentration). A homogeneous, transparent solution was achieved by dissolving PVDF at 60°C for 6 h in a hermetically sealed glass flask, under continuous stirring with a magnetic stirrer. The solution was kept at the intended crystallization temperature for 30 min, which was sufficient for thermal equilibrium. Then, it was deposited by means of drop-casting onto a previously cleaned glass substrate on a temperature-controlled hot plate. The evaporation rate of the solvent during crystallization was determined *in situ* with lever system for force (weight) transmission from the hot plate to a semianalytic balance (Kern, model 440-21A) at a resolution of 0.001 g. The system was arranged so as to minimize the influence of air flow on the balance during the measurement, and it was calibrated for detecting masses to an accuracy of ±0.01 g and could keep the temperature within ±1°C of the intended temperature.

Fourier-Transform InfraRed spectroscopy with Attenuated Total Reflectance (FTIR-ATR) of the films were taken with a spectrometer (Bruker Optics, model Alpha) with resolution of 4 cm^{-1}. The sample was pressed with a controlled pressure onto a Ge (Germanium) crystal, minimizing the effect of surface wrinkling and porosity. All the experiments were performed at room temperature (approximately 22°C), at a relative humidity between 15 and 25% and at atmospheric pressure between 1009 and 1023 mbar.

RESULTS AND DISCUSSION

Influence of the solution concentration on the solvent evaporation rate

The evaporation rate of a solvent depends not only on intrinsic characteristics, such as boiling point and viscosity, but also on external factors including temperature, pressure and concentration of the vapor phase. Figure 1(a) shows the time dependence of the mass loss (i.e., the transition from the liquid to the vapor (gas) phase) per area for different temperatures of the solvent DMF. The mass loss decreases practically linearly at a given temperature, which indicates a constant evaporation rate (*R*) that increases with temperature as shown in Figure 1(b). For pure DMF, *R* lies between -4.2×10^{-4} kg s^{-1} m^{-2} (at 60°C) and -4.1×10^{-3} kg s^{-1} m^{-2} (at 120°C). The inflection of the curves near zero mass in Figure 1(a) indicates that the evaporation is faster in some areas than in others. Therefore, the evaporation rates quoted here are average values for an area of approximately 20 cm^2. Nevertheless, the strong inflection means that the experimental result came close to the ideal situation of uniform evaporation.

For a molecule to leave the surface of a material, the normal component of its velocity must result in a kinetic energy that is larger than the intermolecular bonding. Evaporation is favored at increased temperatures (i.e., at higher average kinetic energies of the solvent molecules) and results in a loss of internal energy from the solution. However, in our experiment, the internal energy was replenished by the heating system, which kept the temperature constant.

The evaporation process of a solvent from a polymer solution can be divided into two stages.[15] In the first stage, the solution is rich in solvent, and the

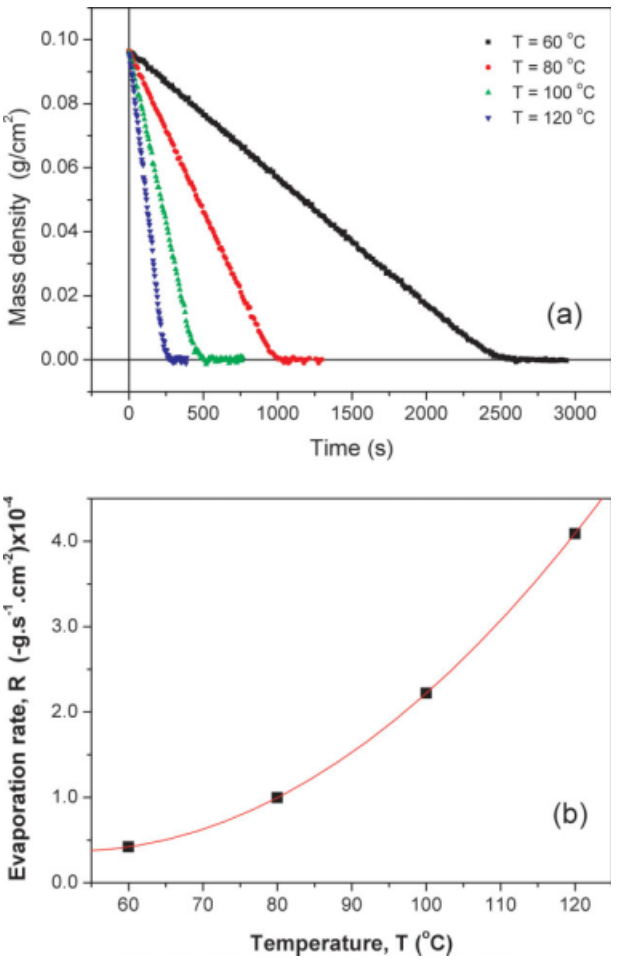

Figure 1 Time dependence of the DMF mass–density loss at different temperatures (a) and temperature dependence of the DMF evaporation rate (b). [Color figure can be viewed in the online issue, which is available at www.interscience.wiley.com.]

mass of the solvent decreases linearly. It is fast because the solvent evaporation rate is high, being practically the same as for the pure solvent, regardless of the (relatively small) fraction of polymer. During this fast regime, the solvent concentration at the air–solution interface and the solvent diffusion coefficient are high, and the evaporation rate is dominated by the solvent diffusion coefficient. In the second stage, the diffusion coefficient decreases significantly with the decrease in the weight fraction of the solvent. The diffusion coefficient decreases because of the microstructure evolution through phase separation. Diffusion becomes very slow, with an insufficient availability of solvent to sustain constant evaporation at the air–solution interface, which results in a loss of the linearity. The reduction in solvent fraction or increase in concentration close to the air interface also causes the partial vapor pressure of the solvent to decrease. This decrease leads to a growing reduction of the evaporation rate and thus to the observed deviation from the linearity. In this regime, evaporation is limited by the diffusion of solvent to the interface. The higher the initial concentration of the solution, the longer is the second evaporation stage. The transition from the first to the second stage is characterized by a time t_c at which the evaporation rate starts to decrease. t_c decreases with the increase of the initial concentration of the solution.

A typical example of the behavior discussed above is illustrated in Figure 2, which depicts the mass loss per area (mass–density loss) for PVDF/DMF solutions with different concentrations at 80°C. A linear behavior is observed at low concentrations, but deviations are apparent at higher concentrations. Comparison with Figure 1(a), where inhomogeneities in the evaporation area were inferred, indicates that other factors than the concentration also affect the evaporation rate.

Figure 3 shows the time derivative of the PVDF + DMF 20 wt % curve from Figure 2. At times below about 140 s, the evaporation rate is constant, which indicates that the diffusion of solvent in the solution is sufficient to compensate the mass loss due to solvent evaporation (first stage). At longer times, the evaporation rate begins to decrease, as the effect from an increased concentration becomes larger than the solubility effect. Then, solvent diffusion decreases considerably because of an increased phase separation (second stage). A turning point appears in Figure 3 at a time of almost 1000 s, which results from a decrease in the evaporation area. At times above 1000 s, two factors contribute to a decrease of the evaporation rate, namely the increase in concentration and the decrease in evaporation area. The latter was also observed by visual inspection of the solution during the crystallization process at times around 1000 s.

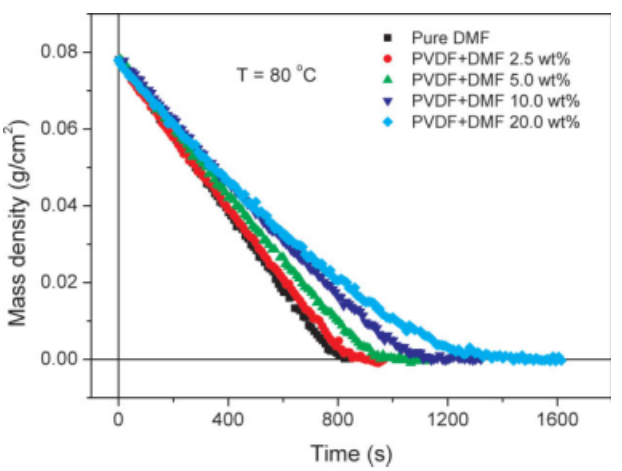

Figure 2 Mass loss per area of a PVDF + DMF solution for different concentrations at a temperature of 80°C. [Color figure can be viewed in the online issue, which is available at www.interscience.wiley.com.]

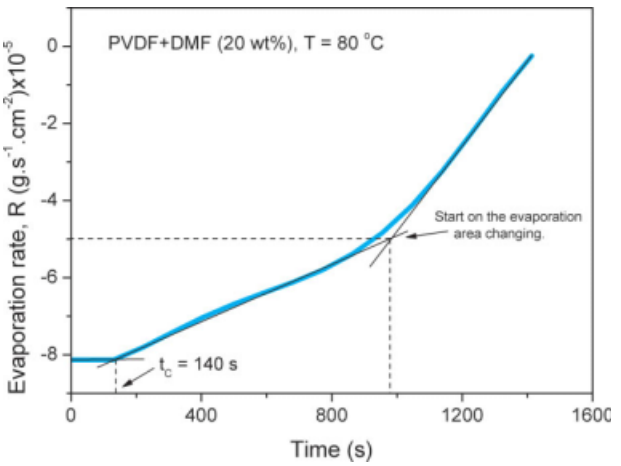

Figure 3 Time derivative of the curve for PVDF + DMF 20 wt % from Figure 2. [Color figure can be viewed in the online issue, which is available at www.interscience.wiley.com.]

The aforementioned results show that the PVDF solution reached the saturation of 23 wt % at t_c = 140 s, i.e., the initial concentration was very close to the critical concentration, above which phase separation could occur. If we take 23 wt % as the critical concentration, for distinct concentrations t_c is estimated as 735 s at 2.5 wt %, 720 s at 5.0 wt %, and 588 s at 10.0 wt % for a crystallization temperature of 80°C. The results in Figure 2 illustrate that R remains constant below t_c (concentration lower than 23 wt % of PVDF) but is concentration dependent.

Figure 4(a,b) represents the behavior of the evaporation rate during the first stage for solutions with different concentrations. Between 60 and 120°C, the relative decrease of the evaporation rate with concentration was always practically the same. The evaporation rate for the polymer solution with the highest concentration (20% of PVDF) is 60–70% of the evaporation rate for pure DMF at all temperatures. However, the evaporation rate is much higher at higher temperatures. For instance, $R = -1.5 \times 10^{-4}$ kg s^{-1} m^{-2} at 120°C, close to four times the value at 60°C. At low temperatures, the solvent diffusivity is practically constant, which means that the rate of sample crystallization is uniform throughout the bulk. In contrast, the concentration affects the diffusivity of the solvent in the dispersed phase at high temperatures, and the evaporation rate grows faster than the solvent diffusivity through the polymeric solution. Hence, the evaporation rate is lower than for the pure solvent because not enough solvent reaches the solution/air interface. Thus, the solution concentration at the top surface increases at high temperatures, which favors thin-layer crystallization at the surface, yet another factor for decreasing the evaporation rate.

Influences of the evaporation rate and of the film thickness on the β-phase fraction

It has previously been shown that the formation of β PVDF depends on the evaporation rate.[9] Therefore, a similar influence is expected from the sample thickness. The FTIR-ATR spectra in Figure 5 were obtained on the upper surface of thin (10–12 μm) films prepared by means of crystallization at various evaporation rates (R). Identical spectra were obtained for the bottom surfaces of the same samples (not shown), indicating that the crystalline phase across the sample is uniform in thin films. One recalls that the penetration depth of infrared (IR) light in polymers lies between 0.1 and 5 μm, depending on the respective wavenumber. Hence, the maximum penetration of the IR beam is approximately half the sample thickness.

The relative β-phase fraction of each sample, $F(\beta)$, was estimated using a procedure analogous to that of Osaki and Kotaka,[16] where the IR absorption is

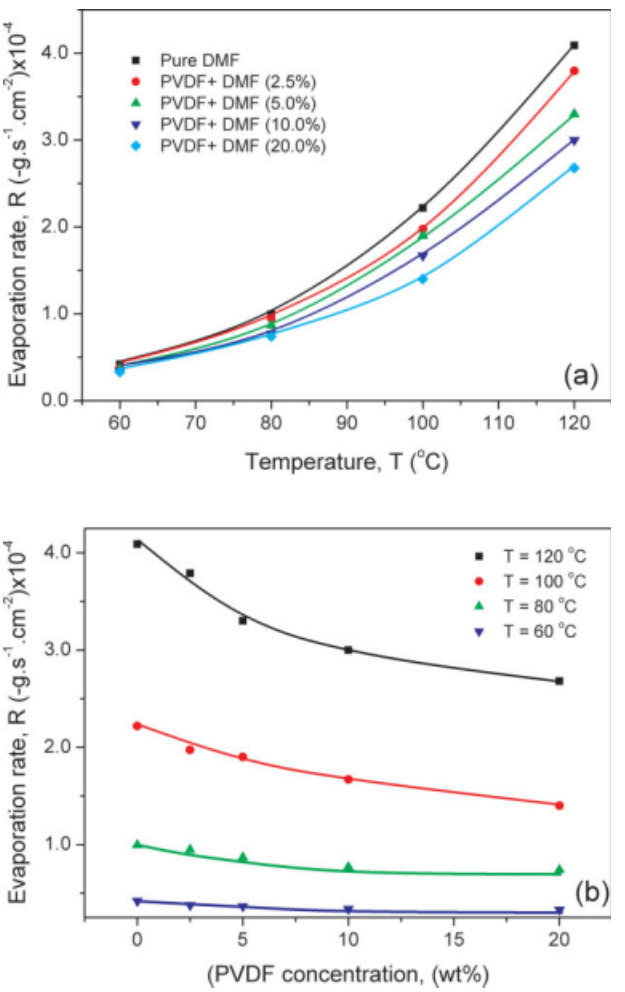

Figure 4 The evaporation rate of PVDF + DMF solutions as function of temperature (a) and of solution concentration (b). [Color figure can be viewed in the online issue, which is available at www.interscience.wiley.com.]

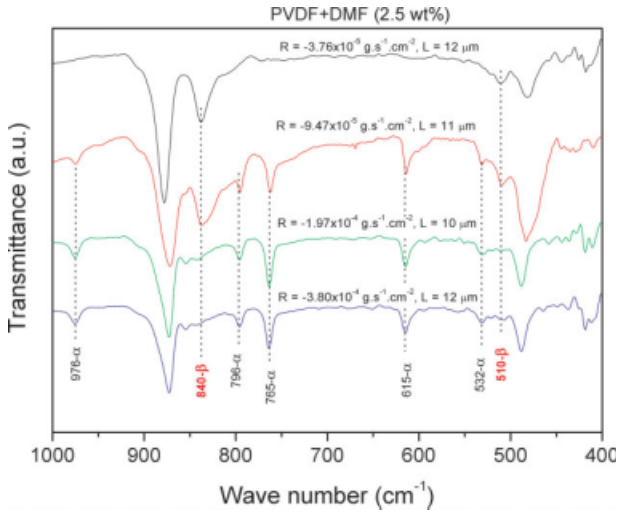

Figure 5 FTIR-ATR spectrograms for the upper surface of thin PVDF samples crystallized at different evaporation rates, R, starting from PVDF + DMF solutions of 2.5 wt %. [Color figure can be viewed in the online issue, which is available at www.interscience.wiley.com.]

assumed to follow the Lambert-Beer law. $F(\beta)$ in a sample containing both phases can be written as follows:

$$F(\beta) = \frac{A_\beta}{1.3A_\alpha + A_\beta} \quad (1)$$

in which A_α and A_β are the ratios of incident and absorbed intensity at 765 and 840 cm^{-1}, respectively, and the constant factor 1.3 was obtained from the absorption coefficient rate K_β/K_α at the corresponding wavenumber.[9]

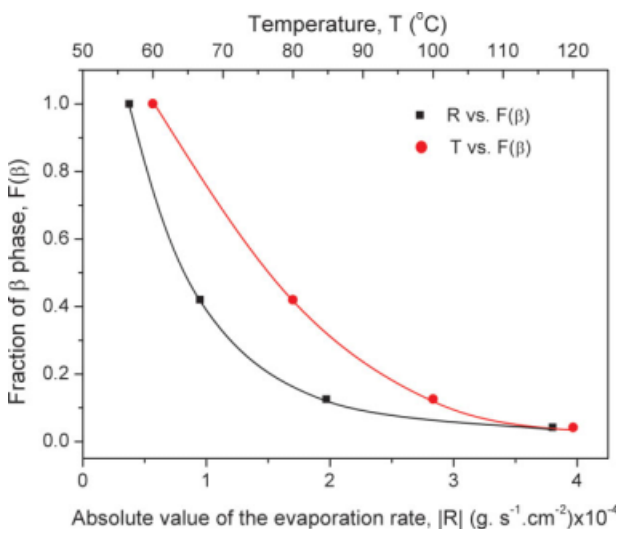

Figure 6 Fraction of β phase, $F(\beta)$, as a function of the solvent-evaporation rate and the crystallization temperature for initial solution concentrations of 2.5 wt % of PVDF + DMF. [Color figure can be viewed in the online issue, which is available at www.interscience.wiley.com.]

The relative β-phase fraction decreases sharply with both the temperature and the evaporation rate, as shown in Figure 6. Although a similar temperature dependence had already been observed by Gregorio and Cestari,[9] the results that were obtained in the present study point to the evaporation rate as another important factor.

For thicker PVDF films, the FTIR-ATR spectra for the top surface are no longer with the same as those for the bottom surface, as illustrated in Figure 7(a,b), respectively. The spectra are identical for the top surfaces, regardless of the sample thickness, but the same does not apply for the bottom surfaces. For the latter, the band at 840 cm^{-1}, assigned to the β phase, increases with thickness, whereas the band at 763 cm^{-1} (characteristic of α phase) decreases with thickness.

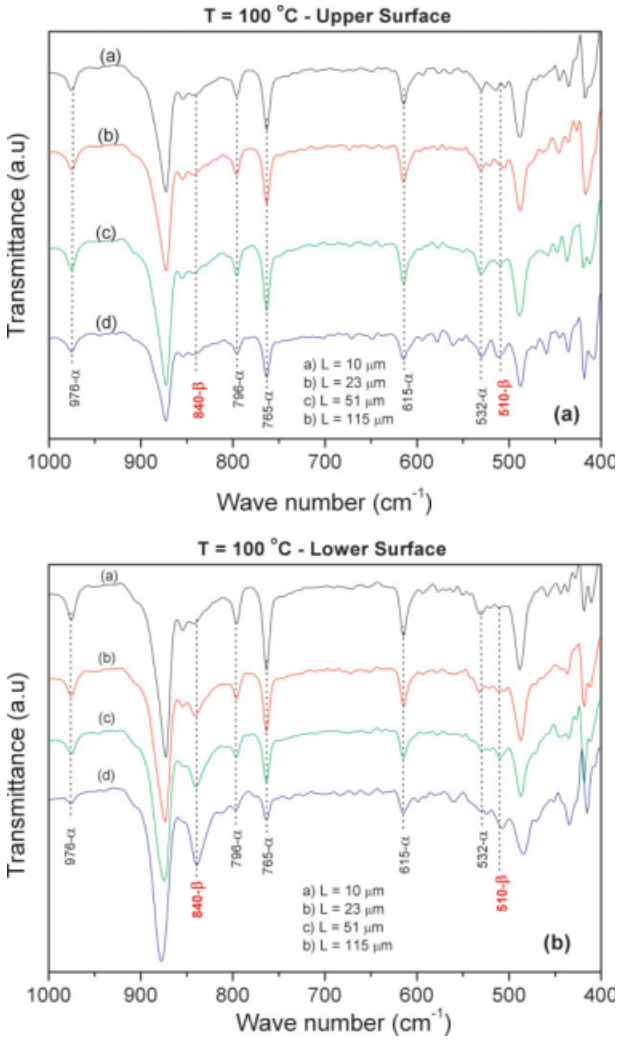

Figure 7 FTIR-ATR results for different sample thicknesses, after crystallization at $R \approx -1.5 \times 10^{-3}$ kg s^{-1} m^{-2} at 100°C. (a) Upper sample surface and (b) lower sample surface. [Color figure can be viewed in the online issue, which is available at www.interscience.wiley.com.]

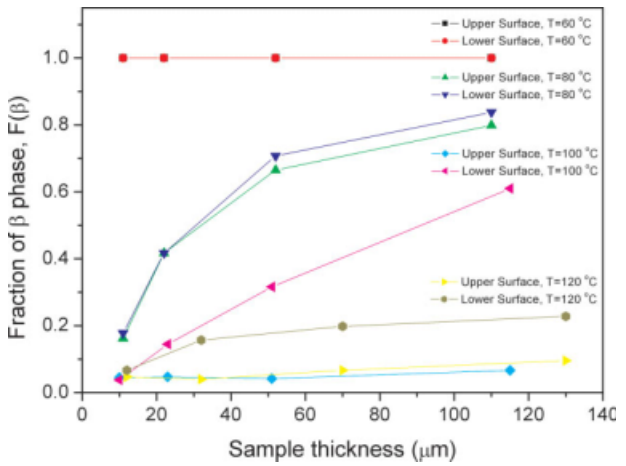

Figure 8 Sample thickness dependence of the β-phase fraction at different crystallization temperatures. [Color figure can be viewed in the online issue, which is available at www.interscience.wiley.com.]

The change in the β-phase fraction with sample thickness is depicted in Figure 8, for various temperatures (the complete spectra from which the data were extracted are not shown). At low temperatures, ($T = 60$°C) and low evaporation rates, the β-phase fraction does not depend on film thickness and is the same at the top and bottom surfaces because of a uniform solvent evaporation rate across the sample volume. In contrast, at $T = 80$°C, the fraction of the β phase increases strongly with film thickness, being slightly higher at the bottom surface. At 100 and 120°C, the β-phase fraction is considerably higher at the bottom surface. This observation is attributed to higher evaporation rates at the upper sample surface, which crystallizes first, thus favoring the formation of the α phase. These results are consistent with those of Gregorio and Borges.[10] The increase in the β-phase fraction with sample thickness at the bottom surface is explained by the low solvent diffusion. If no temperature gradient in the solution is assumed, the data in Figure 8 clearly indicate that the temperature is not the only factor in β-phase formation during PVDF crystallization.

The rationale for explaining the formation of distinct fractions of β phase is as follows: the slow crystallization of a dilute solution leads to the thermodynamically more stable form (i.e., the β phase), whereas the fast crystallization of a concentrated solution is dominated by the kinetics and yields the metastable α phase. This less stable form crystallizes preferentially only at high or at least moderate concentrations.[17] During the first evaporation stage, with practically constant evaporation rates, the increase in concentration (and viscosity) induces a lower polymer-chain mobility and leads to nucleation which occurs in the stable β phase when the crystallization is slow, i.e., at low evaporation rates. At high evaporation rates (high temperatures), there is not enough time for nucleation of the more stable phase and growth of the metastable phase (α) is observed. Therefore, the nucleation of each phase depends on the crystallization rate (or the evaporation rate) during the first stage, and crystal growth occurs during the whole evaporation process.

At low temperatures ($T < 80$°C) or for small sample thicknesses, phase formation depends only on the evaporation rate, which is the same at the two film surfaces. On increasing the temperature, evaporation becomes so fast that a thin PVDF layer crystallizes in the metastable (α) phase near the polymer–air interface. In a thick PVDF film, solvent diffusion in this layer is reduced and so is the rate of crystallization throughout the sample bulk. This leads to increased nucleation and growth of the stable β phase. Consequently, the formation of each phase depends also on the respective position inside the sample.

The formation of the β phase at the bottom surface with increasing temperature is caused by the crystallization at the top surface, which in turn reduces the diffusion of the solvent and therefore decreases the crystallization rate even at the bottom surface. At low temperature (60°C), the evaporation rate during the first stage is low and uniform across the sample, which predominantly leads to the formation of the β phase, regardless of the sample thickness. In contrast, at high temperatures, the high evaporation rates during the first stage cause crystallization of a thin layer at the upper surface, thus reducing solvent diffusion through the sample and the evaporation rate. This is the reason for the differences in evaporation rate between the top and bottom surfaces, with the formation of distinct phases in different locations across the sample. Obviously, the larger the sample thickness, the stronger is this effect.

CONCLUSIONS

The initial evaporation rate of PVDF/DMF solutions is more strongly influenced by the temperature than by the solution concentration. However, at a given temperature, the time period during which the evaporation rate remains constant depends strongly on the solution concentration. More concentrated solutions have lower evaporation rates. The formation of the α and β phases depends basically on the evaporation rates during crystallization even for a concentration well below saturation. Low evaporation rates favor nucleation and growth of the thermodynamically stable β phase, whereas high evaporation rates yield the metastable α phase.

For thick samples, the evaporation rate varies along the bulk. Consequently, the respective formation of the two phases depends on the sample position. The evaporation rate and the distribution of the α and β phases in thick samples varies across the film thickness.

It is during nucleation, when the concentration of PVDF in the solution is still low, that the evaporation rate affects the final phase. When the PVDF concentration increases during the process and growth takes place, there nuclei are already in the phase determined by the initial evaporation rate. This is perhaps the most important conceptual difference from earlier work. The competition in the formation of the α and β phases does not occur during the whole crystallization process, as the distinct, constant evaporation rates during nucleation are important for leading to different relative amounts of the crystalline phases. The possible control in obtaining α and β phases in the same sample, as discussed here, may be exploited in devices where some regions are required to exhibit rather strong piezoelectricity (or pyroelectricity), whereas other regions should be inactive.

References

1. Nagai, M.; Nakamura, K.; Uehara, H.; Kanamoto, T.; Takahashi, Y.; Furukawa, T. J. Polym Sci Part B Polym Phys 1999, 37, 2549.
2. Robinson, S.; Preston, R.; Smith, M.; Millar, C. IEEE Trans UFFC 2000, 47, 1336.
3. Lovinger, A. J. In Developments in Crystalline Polymers, Bassett, D. C., Ed.; Applied Science Publishers Ltd.: London, 1982; p 195.
4. Davies, G. R.; Singh, H. Polymer 1979, 20, 772.
5. Hsu, T. C.; Geil, P. H. J Mat Sci 1989, 24, 1219.
6. Branciforti, M. C.; Sencadas, V.; Lancero-Mendez, S.; Gregorio, R., Jr. J Polym Sci Part B Polym Phys 2007, 45, 2793.
7. Davis, G. T.; McKinney, J. E.; Broadhurst, M. G.; Roth, S. C. J Appl Phys 1978, 49, 4998.
8. Yang, D.; Chen Y. J Mater Sci Lett 1987, 6, 599.
9. Gregorio, R., Jr; Cestari M. J Polym Sci Part B Polym Phys 1994, 32, 859.
10. Gregorio, R., Jr; Borges, D. S. Polymer 2008, 49, 4009.
11. Salimi, A.; Yousefi, A. A. J Polym Sci Part B Polym Phys 2004, 42, 3487.
12. Benz, M.; Euler, W. B. J Appl Polym Sci 2003, 89, 1093.
13. Boccaccio, T.; Bottino, A.; Capannelli, G.; Piaggio, P. J Membr Sci 2002, 210, 315.
14. Kim, K. M.; Jeon, W. S.; Park, N.-G.; Ryu, K. S.; Chang, S. H. Korean J Chem Eng 2003, 20, 934.
15. Guerrier, B.; Bouchard, C.; Allain, C.; Bérnard, C. AIChE J 1998, 44, 791.
16. Osaki, S.; Kotaka, T. Ferroelectrics 1981, 32, 1.
17. Threlfall, T. Org Process Res Dev 2000, 4, 384.